Research Square

Preprints are preliminary reports that have not undergone peer review.
They should not be considered conclusive, used to inform clinical practice,
or referenced by the media as validated information.

Numerical Evaluation and Probabilistic Calibration of Constitutive Models for Tunnelling in Weak Rock Masses: A Case Study from the Honaz Tunnel, Türkiye

Ertuğrul Karakaplan

ekarakaplan@pau.edu.tr

Pamukkale University

Devrim Alkaya

Pamukkale University

Research Article

Keywords: Constitutive models, Tunnel convergence, Probabilistic risk assessment, Monte Carlo simulation, Weak rock masses

Posted Date: April 30th, 2026

DOI: https://doi.org/10.21203/rs.3.rs-8340182/v1

License: This work is licensed under a Creative Commons Attribution 4.0 International License.
Read Full License

Additional Declarations: No competing interests reported.

Version of Record: A version of this preprint was published at Geotechnical and Geological Engineering on September 29th, 2026. See the published version at https://doi.org/10.1007/s10706-026-03923-y.

Numerical Evaluation and Probabilistic Calibration of Constitutive Models for Tunnelling in Weak Rock Masses: A Case Study from the Honaz Tunnel, Türkiye

ABSTRACT

This study evaluates the mechanical behaviour of weak rock masses along the Honaz Tunnel (SW Türkiye) by combining field-calibrated 2D finite-element simulations (RS2) with a probabilistic risk assessment. Three constitutive criteria — Mohr-Coulomb (MC), Hoek-Brown (HB) and Generalized Hoek-Brown (GHB) — were compared under supported excavation scenarios. Support layouts were derived from six empirical classification systems (Q, RMR, RMQR, RMi, RSR, NATM) and numerical predictions were benchmarked against in-situ convergence measurements. The MC model provided the best fit to field data ($R^2 = 0.94$), while HB/GHB tended to overestimate deformations in the weakest units. To account for parameter uncertainty, we performed Monte Carlo simulations (45,000 runs) using an analytical elastoplastic tunnel solution implemented in MATLAB. Results indicate that shallow very-weak units show limited stress-induced convergence due to low confinement, whereas a deeper transition unit (Calcareous Quartz Schist) exhibited the highest failure probability (≈0.2%) and the lowest reliability index ($\beta = 5.59$). The findings highlight the effectiveness of a hybrid deterministic–probabilistic workflow for robust tunnel design in heterogeneous weak rock masses.

Keywords: Constitutive models; Tunnel convergence; Probabilistic risk assessment; Monte Carlo simulation; Weak rock masses.

1. INTRODUCTION

Recent tunnel projects in weak and highly heterogeneous rock masses face significant uncertainty in support design due to spatial variability of geomechanical parameters. Deterministic numerical models alone may either underestimate squeezing risk or produce overly conservative designs. This study addresses that gap by integrating field-calibrated FE modelling with probabilistic risk quantification.

The design of underground structures in geotechnically challenging environments requires a robust understanding of rock mass behavior and the interaction between the ground and support systems. Numerical modeling has become an indispensable tool in geotechnical engineering for simulating complex stress-strain conditions (Jing 2003; Terron-Almenara et al., 2023). Recent studies have demonstrated the effectiveness of finite element methods in evaluating tunnel stability in weak rock masses (Zhang et al., 2024; Boukarm et al., 2024). The integration of empirical rock mass classification systems with numerical modeling approaches has proven essential for reliable support design, particularly in heterogeneous geological conditions (Terron-Almenara et al., 2025; Mushahary et al., 2020). Furthermore, comparative analyses of different constitutive models, including Mohr-Coulomb and Hoek-Brown formulations, have provided valuable insights into the mechanical behavior of weak rock masses under complex stress states (Saeidi et al., 2022). However, the reliability of these models depends heavily on the selection of an appropriate constitutive model and the accurate characterization of rock mass properties. This is particularly critical for tunnels excavated in weak rock masses, which are characterized by low strength, high deformability, and significant spatial variability (Hoek and Marinos 2000).

In conventional practice, tunnel support design often relies on deterministic analyses using mean values of geomechanical parameters. However, such approaches fail to capture the inherent uncertainty and spatial variability of rock masses, potentially leading to either unsafe or overly conservative designs. While empirical classification systems (e.g., Q, RMR, NATM) provide practical guidelines, their integration with numerical modeling and probabilistic risk assessment remains a developing field, especially for complex geological settings involving weak rocks.

Although previous studies compared constitutive laws for rock tunnelling, few have combined field calibration, multiple classification-based support designs and a large-scale Monte Carlo reliability analysis on a single case study. The Honaz Tunnel, a critical component of the Denizli–Antalya highway in Türkiye, traverses challenging ground conditions, including highly fractured conglomerates, fault breccia, and slope debris. This study presents a comprehensive investigation that bridges the gap between deterministic numerical modeling and probabilistic risk analysis. The primary objectives are: (1) to evaluate the performance of three failure criteria (Mohr-Coulomb, Hoek-Brown, and Generalized Hoek-Brown) through field calibration; (2) to assess the effectiveness of support systems designed according to six empirical classification systems; and (3) to quantify the deformation risk and reliability of support systems using Monte Carlo simulations, thereby addressing parameter uncertainty. This research aims to provide a robust, multi-faceted framework for tunnel design in weak rock conditions by validating numerical predictions with in-situ measurements and statistical analysis.

2. GEOLOGICAL AND GEOTECHNICAL SETTING

The Honaz Tunnel is situated in the tectonically active southwestern region of Türkiye, within the Menderes Massif. The tunnel alignment, spanning approximately 2,540 meters, traverses a highly complex geological environment characterized by intensive faulting, heterogeneous lithologies, and significant alteration zones (Fig. 1). The excavation encounters a challenging matrix where competent limestone blocks are frequently embedded within weathered and clay-altered weak materials, creating abrupt changes in stiffness and strength that complicate support design.

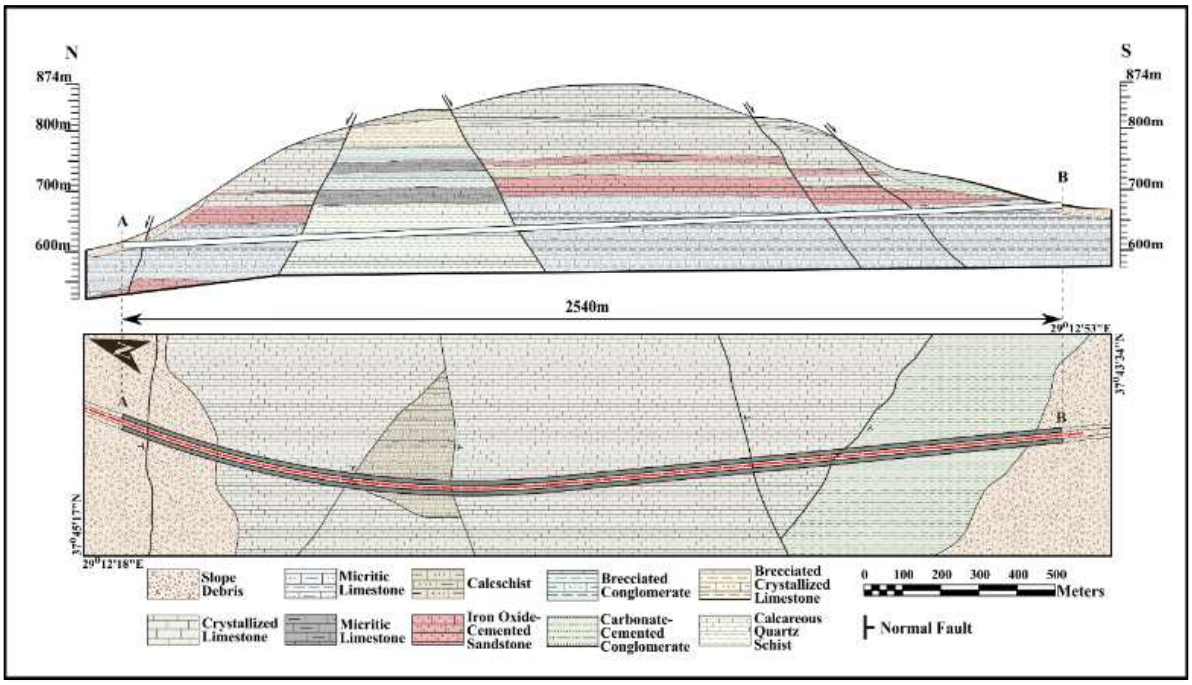


Fig. 1. Geological cross-section of the Honaz Tunnel route.

The lithological profile is dominated by micritic and crystalline limestone, conglomerate, sandstone, slope debris, and fault breccia. While the limestone formations (Units S1-S3) represent the most competent units, their mechanical integrity is often compromised by intense tectonic jointing. Conversely, the sedimentary units, specifically the conglomerate and sandstone (Units S6-S7), are weakly cemented and exhibit high deformability. The poorest ground conditions are observed in the slope debris (S8) and fault breccia (S9) zones, which display extremely low shear strength and weak rock mass behavior, necessitating robust and immediate support measures to control convergence.

To characterize the engineering behavior of these heterogeneous materials, an extensive site investigation and laboratory testing program was conducted. The testing program included determination of Uniaxial Compressive Strength (UCS), Brazilian Tensile Strength (BTS), Point Load Index ($I_{s(50)}$), as well as the derivation of cohesion (c) and friction angle (φ) using empirical failure criteria based on the intact rock properties. Crucially, to address the spatial variability inherent in weak rock masses, the geomechanical parameters were analyzed statistically. Table 1 summarizes the mean values of the physico-mechanical properties for the nine identified lithological units. These mean values served as the baseline for the deterministic numerical calibration, while the statistical dispersion (standard deviation) of these parameters was utilized to define the probability distributions for the Monte Carlo risk assessment presented later in this study.

Table 1

Summary of mean geomechanical properties of the rock units derived from laboratory testing.

Rock mass number		S1	S2	S3	S4	S5	S6	S7	S8	S9
Uniaxial compressive strength – UCS	MPa	48.81	24.71	39.40	41.49	11.67	22.17	2.05	0	0
Cohesion – c	MPa	1.81	1.72	2.01	2.09	1.82	1.29	0.28	0.1	0.1
Angle of internal friction – φ	Deg.	38	44	40	39	27	28	25	22	24
Brazilian tensile strength – BTS	MPa	0.27	0.48	0.41	0.42	1.13	0.30	0.15	0	0
Point load strength – $I_{s(50)}$	MPa	2.72	3.08	2.63	2.44	1.39	2.22	0.17	0	0
Poisson's ratio – υ	-	0.31	0.27	0.29	0.30	0.38	0.37	0.39	0.41	0.40
Density – ρ	t/m^3	2.68	2.65	2.65	2.60	2.42	2.72	2.30	1.80	1.90
Schmidt hardness – N	-	32	29	31	30	15	20	-	-	-
Porosity – n	%	1.08	1.10	2.39	1.87	5.21	1.87	-	-	-
Young's modulus of intact rock – E	MPa	4757	3880	3164	3436	1128	2366	-	-	-
Rock mass deformation modulus – E_m	MPa	3134	2139	3984	1747	978	1141	675	418	505
Average depth	m	150	150	200	150	150	150	30	15	30

In addition to laboratory data, the rock masses were classified in situ using six empirical systems: Q-system (Q) (Barton et al., 1974; Barton 2002), Rock Mass Rating (RMR) (Bieniawski 1989), Rock Mass Quality Rating (RMQR) (Aydan et al., 2014), Rock Mass index (RMi) (Palmström 1995), Rock Structure Rating (RSR) (Wickham et al., 1972), and the New Austrian Tunnelling Method (NATM) (Rabcewicz 1964). The classification results, presented in Table 2, highlight the significant variation in rock mass quality, ranging from "Fair" in limestone units to "Extremely Poor" in fault zones.

Table 2

Rock mass classification results based on empirical systems.

Unit ID	Rock mass units	Q	RMR	RMQR	RMi	RSR	NATM	RQD	GSI
S1	Micritic limestone	1.32	40	42	0.286855	48	B2	10	35
S2	Micritic limestone	0.528	35	32	0.051981	45	B3	12	30
S3	Crystalline limestone	4.752	44	49	0.89687	58	B2	18	39
S4	Brecciated crystalline limestone	0.176	30	35	0.141006	43	B3	10	25
S5	Calcareous quartz schist	0.010417	24	22	0.024813	36	C2	6	23
S6	Iron oxide cemented sandstone	0.020833	27	25	0.002909	38	C2	5	22
S7	Carbonate cemented conglomerate	0.007333	17	17	0.010214	27	C3	3	16
S8	Slope debris	0.0022	10	10	0.000202	20	C4	1	8
S9	Fault breccia	0.0055	13	14	0.000341	22	C4	1	11

These geotechnical characterizations define the physical boundaries of the tunnel environment and provide the necessary input data for both the field-calibrated deterministic models and the probabilistic reliability analyses conducted in this research.

3. METHODOLOGY

This study employs a hybrid methodological framework combining deterministic finite element modeling (FEM) with probabilistic risk assessment. The workflow consists of three phases: (1) Field-calibrated numerical simulations using RS2 to evaluate constitutive model performance; (2) Comparative analysis of empirical support designs; and (3) Probabilistic reliability analysis using Monte Carlo simulations to quantify risks associated with parameter variability.

3.1. Theoretical Background of Numerical Analysis

RS2 model details: Plane-strain 2D RS2 (v.11 - Rocscience, 2021) models used triangular 3-node elements; minimum element size ~D/50 around the tunnel; boundary at 5D to avoid reflections. Gaussian elimination solver selected. Mesh convergence tests were performed (element refinement until crown convergence change < 2%). Elastic-plastic analyses used associated flow rule and small-strain assumption.

Field calibration procedure: (1) initial parameters from lab tests (Table 1); (2) iterative tuning of Em and joint parameters to match measured crown convergences at three monitoring sections; (3) calibration accepted when simulated vs measured residuals fell within ±10% of measured convergence.

3.2. Numerical Modeling Framework for Tunnel Excavation and Support

Two-dimensional (2D) plane-strain analyses were conducted to simulate the sequential excavation and support installation. To eliminate boundary effects, the model boundaries were extended to a distance of five times the tunnel diameter from the excavation center. The domain was discretized using a graded mesh of 3-noded triangular elements, optimized to balance computational efficiency with result accuracy near the excavation zone. The excavation followed the NATM principles, simulated in a staged sequence:

1. Stress Initialization: In-situ stresses were applied based on overburden depth and rock mass unit weight.
2. Top Heading Excavation: Upper half excavation followed by immediate relaxation.
3. Bench Excavation: Lower half excavation.
4. Support Installation: Shotcrete, bolts, and steel sets were activated immediately after each stage to simulate ground-support interaction.

3.3. Material Failure Models

Three constitutive models were evaluated using parameters derived from Tables 1 and 2. The specific formulations are described below.

3.3.1. Hoek-Brown Material Model

The Hoek-Brown failure criterion is one of the most widely used material models for simulating rock mass behavior. Initially proposed by Hoek and Brown (1980a, 1980b) for the design of underground excavations in intact rock, it was developed based on brittle failure studies in rock by Hoek (1968) and empirical observations of jointed rock masses by Brown (1970). The model begins with the properties of intact rock and incorporates reduction factors that reflect the influence of joints and discontinuities, adapting the behavior to rock mass conditions.

The general form of the Hoek-Brown failure criterion in terms of principal stresses is given as:

$$F_s = \sigma_1 - \sigma_3 - \sigma_{ci}\left(m\frac{-\sigma_1}{\sigma_{ci}} + s\right)^{0.5} = 0 \quad (1)$$

where "σ_{ci}" is the uniaxial compressive strength of intact rock, "m" is a reduced material constant derived from "m_i" (for intact rock), and "s" is a constant with a maximum value of "1" for intact rock.

Key mechanical characteristics modeled using the Hoek-Brown criterion include:

- Nonlinear shear strength behavior dependent on the confining stress
- Tensile strength
- Dilation and critical state failure behavior
- Lode angle (equation 2) dependency of shear strength

The dependency on the Lode angle can be expressed as:

$$L = \frac{2\sigma_2 - \sigma_1 - \sigma_3}{\sigma_1 - \sigma_3} \quad (2)$$

Compared to the linear Mohr-Coulomb model, the Hoek-Brown model offers a more realistic representation of strength at varying stress levels, especially in high-stress or fractured conditions, making it suitable for geotechnical and mining stability assessments. It also performs reliably in load-displacement analyses involving both rock material and rock masses.

3.3.2. Generalized Hoek-Brown Material Model

The Generalized Hoek-Brown model introduces an additional parameter, "a", replacing the fixed exponent "0.5", to enhance the model's ability to represent very weak rock masses (Hoek et al., 2002; Hoek and Brown 2019):

$$F_s = \sigma_1 - \sigma_3 - \sigma_{ci}\left(m\frac{-\sigma_1}{\sigma_{ci}} + s\right)^a = 0 \quad (3)$$

The parameters "m", "s", and "a" are derived using the Geological Strength Index (GSI), and the disturbance factor "D", as follows:

$$m = m_i e^{\left(\frac{GSI-100}{28-14D}\right)} \quad (4)$$

$$s = e^{\left(\frac{GSI-100}{9-3D}\right)} \quad (5)$$

$$a = \frac{1}{2} + \frac{1}{6}e^{-GSI/15} - e^{-20/3} \quad (6)$$

3.3.3. Mohr-Coulomb Material Model

The Mohr-Coulomb failure criterion is widely used in geotechnical engineering for soils and rock masses. It assumes a linear relationship between shear strength and normal stress, as first postulated in the Coulomb hypothesis (Coulomb 1776; Mohr 1900; Labuz and Zang 2012).

$$\tau = c - \sigma_n \tan\varphi \quad (7)$$

Here, "τ" is the shear strength, "σ_n" is the normal stress, "ϕ" is the internal friction angle, and "c" is cohesion.

Mechanical behavior captured by the Mohr-Coulomb model includes:

- Isotropic shear strength behavior with cohesion-friction properties that linearly increase with stress
- Tensile strength modeling through a stress-based failure function
- Volume expansion (dilation) or critical state behavior at failure
- Shear strength dependency on the Lode angle (common in granular soils)

While it lacks the nonlinearity of Hoek-Brown, the Mohr-Coulomb model is well-suited for stability analyses of geotechnical and mining problems not involving wide stress ranges. It is also commonly used for load-displacement simulations involving gravels, sands, intact rocks, and rock masses.

When expressed in terms of principal stresses, the Mohr-Coulomb criterion takes the form:

$$F_s = \frac{1}{2}(\sigma_1 - \sigma_3) + \frac{1}{2}(\sigma_1 + \sigma_3)\sin\varphi - \cos\varphi = 0 \quad (8)$$

Crucially, while deterministic models rely on mean parameter values, rock masses exhibit inherent spatial variability. To address this, the study extends beyond standard numerical modeling by integrating a probabilistic framework described in Section 3.5.

3.4. Support System Scenarios

Support systems were designed based on six empirical rock mass classification methods: Q, RMR, RMQR, RMi, RSR, and NATM. The specific design parameters (bolt length, shotcrete thickness, steel ribs) for each rock mass unit are detailed in Table 3. These designs served as variable inputs in the numerical model to evaluate their comparative efficacy in controlling tunnel convergence.

Table 3
Types and quantities of support elements recommended by rock mass classification systems.

System	Rock mass number	Rock bolts Length (m)	Rock bolts spacing (m)	Number of rock bolts	Shotcrete (mm)	Steel rib type or profile (mm)	Steel ribs spacing (m)	Invert lining (mm)	Invert bolt (m)	Wire mesh (mm)	Concrete lining (mm)	Reinforced shotcrete (mm)
Q	S1	3	1.8	20-21	90	-	-	90	3	-	-	-
	S2, S3	3	1.6	22-23	120	-	-	120	3	-	-	-
	S4	3	1.4	27-28	300	16	0.6	300	3	-	-	-
	S5	3	1	36-37	400	20	0.2	400	3	-	-	-
	S6	3	1.1	33-34	450	20	0.2	450	3	-	-	-
	S7	3	1	36-37	550	20	0.15	550	3	-	-	-
	S8	3	0.5	74-75	550	20	0.1	550	3	-	-	-
	S9	3	0.75	49-50	500	20	0.15	500	3	-	-	-
RMR	S1, S2, S4, S5, S6	5	1	27-28	150	Medium	1.5	150	-	6	-	-
	S3	4	1.5	17-18	100	-	-	100	-	6	-	-
	S7, S8, S9	6	1	38-39	200	Heavy	0.75	200	6	6	-	-
RMQR	S1, S3	5	1.5	17-18	150	Medium	1.2	300	-	6	300	-
	S2, S4, S5, S6	6	1	37-38	200	Heavy	1	500	6	6	500	-
	S7, S8, S9	7	0.5	74-75	250	Very Heavy	0.8	800	7	6	800	-
RMi	S1, S3	3	1.25	21-22	100	-	-	100	-	6	-	-
	S2	3	1	27-28	200	-	-	200	-	6	-	-
	S4	3	1.25	21-22	150	-	-	150	-	6	-	-
	S5	3	1	27-28	250	-	-	250	-	6	-	-
	S6	3	0.5	52-53	250	-	-	100	-	6	100	10
	S7, S8, S9	3	0.5	52-53	300	-	-	200	-	6	200	10
RSR	S1	3	1	26-27	90	Heavy	0.6	90	-	-	-	-

	S2	3	0.75	35-36	100	Heavy	0.6	100	-	-	-	-
	S3	3	1	26-27	70	Medium	0.6	70	-	-	-	-
	S4	3	0.75	35-36	110	Heavy	0.6	110	-	-	-	-
	S5	3	0.6	44-45	150	Heavy	0.6	150	-	-	-	-
	S6	3	0.5	52-53	150	Heavy	0.6	150	-	-	-	-
	S7	3	0.5	52-53	200	Heavy	0.6	200	-	-	-	-
	S8, S9	3	0.5	52-53	300	Heavy	0.6	300	-	-	-	-
NATM	S1, S3	4-6	1.25	17-18	250	Light	1	250	-	6	-	-
	S2, S4,	4	1.25	17-18	250	Light	1	250	-	6	-	-
	S5, S6	6-8	1	22-23	300	Medium	0.6	300	-	8	-	-
	S7, S8, S9	6-9	1	24-25	310	Heavy	0.6	310	-	8	-	-

3.5. Probabilistic Risk Assessment Framework

To overcome the limitations of deterministic analysis—specifically the inability to account for parameter uncertainty — a probabilistic risk assessment was conducted using Monte Carlo simulations (MCS). Since running thousands of finite element models is computationally prohibitive, the probabilistic analysis utilized the analytical elastoplastic solution for circular tunnels (Carranza-Torres and Fairhurst 1999; Fama 1993) implemented in a MATLAB environment. This approach allows for the rapid computation of tunnel convergence under stochastic conditions.

The probabilistic framework involved the following steps:

1. Stochastic Definition: Input parameters (UCS, GSI, E_m, c, φ) were defined not as fixed values, but as normal probability distributions characterized by the mean values and standard deviations derived from the site investigation (as detailed in Section 2).
2. Simulation: For each of the nine rock mass units, 5,000 iterations were performed, totaling 45,000 runs. In each iteration, parameters were randomly sampled from their respective distributions.
3. Reliability Analysis: The probability of failure (P_f) was calculated based on the exceedance of a critical strain threshold (1%), and the Reliability Index (β) was computed to quantify the safety margin of each unit.

This dual-approach (Deterministic RS2 + Probabilistic MATLAB) ensures that the findings are robust against both model selection bias and geological uncertainty.

4. RESULT AND DISCUSSION

4.1. Evaluation of Predictive Accuracy Using Regression Metrics

This section presents a comprehensive evaluation of the predictive capabilities of three constitutive models based on different failure criteria, using a robust dataset generated from field-calibrated numerical simulations. The dataset comprises deformation data from nine distinct rock mass units, each numerically analyzed under six empirical rock mass classification-based support schemes (Q, RMR, RMQR, RMi, RSR, and NATM). Among these, the actual support design used during the construction of the Honaz Tunnel served as the reference configuration for numerical calibration. To ensure comparability across all cases, the numerical results were normalized with respect to the NATM-based deformation values by applying scaling coefficients derived from convergence benchmarks observed in situ. This normalization was applied to eliminate scale-dependent biases and to provide a consistent benchmark for comparison. The performance of the models was assessed using statistical indicators including the coefficient of determination (R^2), adjusted R^2 ($A.R^2$), root mean square error (RMSE), mean squared error (MSE), and mean absolute error (MAE), defined by the following equations:

$$R^2 = 1 - \frac{\sum_{i=1}^{N}(y_i - \hat{y}_i)^2}{\sum_{i=1}^{N}(y_i - \bar{y})^2} \quad (9)$$

$$A.R^2 = 1 - (1 - R^2)\frac{n-1}{n-p-1} \quad (10)$$

$$RMSE = \sqrt{\frac{1}{N}\sum_{i=1}^{N}(y_i - y_i^*)^2} \quad (11)$$

$$MSE = \frac{1}{N}\sum_{i=1}^{N}(y_i - y_i^*)^2 \quad (12)$$

$$MAE = \frac{1}{N}\sum_{i=1}^{N}|y_i - y_i^*| \quad (13)$$

While R^2 and Adjusted R^2 quantify the explanatory power of the models, RMSE and MAE provide insight into their absolute predictive accuracy. Notably, RMSE is more sensitive to large deviations due to the squaring of residuals, whereas MAE provides a more conservative assessment of average error, particularly valuable when large residuals may disproportionately influence model evaluation.

4.2. Model Validation Against Field-Measured Deformations

The predictive performance of the numerical models (Mohr-Coulomb (MC), Hoek-Brown (HB), and Generalized Hoek-Brown (GHB)) was evaluated by comparing their simulated total crown convergence against field-monitored convergence data. This direct comparison with in-situ measurements provides a quantitative validation of the models, enhancing the reliability of their application in tunnel design and excavation planning. The correlation between predicted and measured deformations for all supported tunnel sections is presented in Fig. 2.

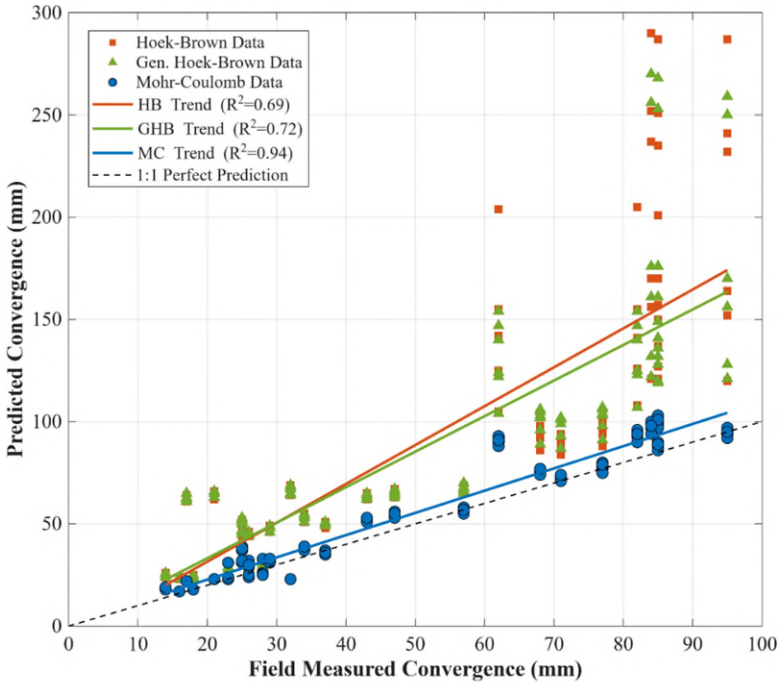


Fig. 2. Correlation between field-measured and numerically predicted crown convergence values.

The Mohr-Coulomb model demonstrated the highest predictive accuracy, achieving an R^2 of 0.94. This suggests that for weak and fractured lithologies encountered in the Honaz Tunnel, a linear failure envelope better captures the prevailing deformation mechanisms. In contrast, the GHB (R^2 = 0.72) and HB (R^2 = 0.69) models notably

overestimated deformation, particularly in the weakest units such as conglomerate and slope debris. The quantitative statistical performance indicators for all three models are summarized in Table 4.

Table 4

Statistical performance indicators for the MC, HB, and GHB models based on field-calibrated convergence data.

Model	R^2	A. R^2	RMSE	MAE	MSE
MC	0.944	0.944	6.13	4.48	37.60
HB	0.690	0.688	14.48	11.56	209.56
GHB	0.720	0.719	13.76	10.72	189.22

The exceptional predictive accuracy of the Mohr-Coulomb model ($R^2 = 0.94$) can be attributed to two key factors: the homogenized behavior of the intensely fractured weak rock mass, which is well-captured by a linear failure criterion, and the use of a robust, comprehensively derived deformation modulus (E_m). The derivation of "E_m", which entailed a systematic analysis of numerous empirical formulas (as presented in the first author's previous work, Karakaplan 2023), provided a realistic input parameter that was critical to the model's performance.

While all three models yielded comparable results in the more competent limestone formations, the Mohr-Coulomb model was the only one to maintain consistent accuracy across all rock mass units, including those exhibiting weak rock mass or heavily jointed behavior. This emphasizes the influence of failure criterion selection on tunnel convergence predictions and supports the use of simpler linear models like MC for highly fractured or weak rock masses. Similar conclusions were reported by Saeidi et al. (2022), who showed that the Mohr-Coulomb model, when compared to the Generalized Hoek-Brown criterion in RS2 simulations, exhibited better performance in predicting tunnel convergences under low-quality rock mass conditions, particularly when GSI variations were significant. MC's superior performance likely stems from the heavily fractured nature of the investigated rock masses where a homogenized linear envelope better represents immediate near-field deformation, whereas HB/GHB capture non-linear strength behaviour under higher confinement.

Therefore, these results strongly advocate for selecting constitutive models that align with the mechanical behavior of specific rock units, even if this means opting for simpler linear models over more complex non-linear ones in specific geotechnical contexts such as the one presented here.

4.3. Assessment of Empirical Support Designs Across Varying Rock Conditions

Numerical simulations were conducted to evaluate the convergence control performance of six empirical support schemes applied across all major rock mass units. Each support system was implemented based on the specific recommendations of the respective classification system, including shotcrete, rock bolts, steel ribs, and concrete lining. Beyond material model performance, the study also focused on the comparative effectiveness of support systems derived from six empirical classification methods: Q, RMR, RMQR, RMi, RSR, and NATM. The predicted convergence values, expressed as a percentage of tunnel diameter, were compared for each support system across varying rock mass qualities.

All support systems significantly reduced convergences in comparison with the unsupported configuration. However, designs based on RMQR, Q, and NATM systems resulted in the most effective control, particularly in weak rock mass units (units 4-9). These results were most pronounced in rock mass units such as slope debris and clayey conglomerate, where convergence tends to peak under insufficient confinement or delayed support installation. In contrast, the RSR-based designs produced the highest convergence levels, particularly in weak ground, primarily due to insufficient reinforcement provisions and overly simplified assumptions regarding rock mass strength. These findings highlight the superiority of updated and more comprehensive classification systems in recommending effective support strategies under challenging geological conditions. The comparative performance of all support systems across the nine rock mass units is visually summarized in Fig. 3. However, relying solely on deterministic values may overlook

critical uncertainties. Therefore, to address the inherent variability of rock mass parameters and enhance design reliability, a probabilistic assessment was conducted, as detailed in the following section.

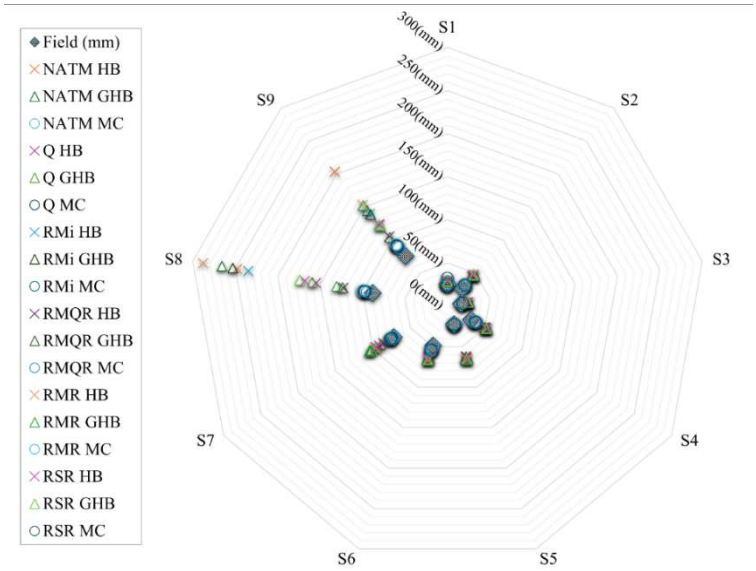


Fig. 3. Support system efficacy: normalized crown convergence by rock mass number and design method.

4.4. Probabilistic Risk Assessment of Critical Sections

In response to the inherent spatial variability of rock mass parameters—a critical limitation noted in deterministic analyses—a probabilistic assessment was conducted using Monte Carlo simulations. Unlike conventional deterministic approaches that rely on mean values, this study treated key input parameters (UCS, GSI, and E_m) as stochastic variables defined by normal distributions with coefficients of variation derived from field data variability. A total of 45,000 simulations (5,000 runs per rock mass unit) were performed using the elastoplastic Mohr-Coulomb analytical solution for a circular tunnel. The statistical distribution of the convergence results for each rock mass unit is visually presented in Fig. 4, while the calculated probabilities of exceeding a critical strain threshold of 1.0% are summarized in Table 5.

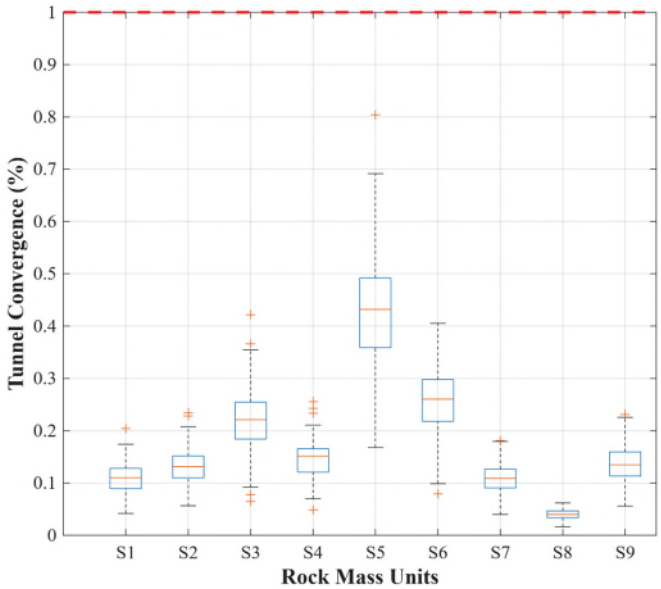


Fig. 4. Box-plot distribution of tunnel convergence for all rock mass units, illustrating the impact of parameter uncertainty on convergence risk.

As illustrated in Fig. 4, the spread of the data (represented by the box-plot whiskers) highlights the significant impact of parameter uncertainty, particularly in unit S5. The analysis reveals a distinct behavior in the transition zones. While the poorest quality rock masses (S8 and S9) exhibit low stress-induced convergence due to shallow overburden (low confinement), the Calcareous Quartz Schist (S5) unit presents the highest probabilistic risk (lowest Reliability Index, $\beta = 5.59$), with a mean convergence of 0.43% and a notable probability of exceeding critical limits. This suggests that for units like S5, standard support designs based solely on mean parameters may underestimate the risk of squeezing, necessitating a more conservative support strategy compared to shallower, albeit weaker, units.

Table 5

Summary of probabilistic convergence analysis and reliability indices for each rock unit (based on 45,000 Monte Carlo simulations).

Unit ID	Rock mass units	Field measured convergence (%)	Deterministic mean convergence (%)	Probabilistic mean convergence (%)	Max convergence (P99) (%)	Probability of failure (%)	Reliability index
S1	Micritic limestone	0.26	0.28	0.11	0.16	0.00	51.99
S2	Micritic limestone	0.27	0.40	0.13	0.20	0.00	41.50
S3	Crystalline limestone	0.16	0.22	0.22	0.34	0.00	21.36
S4	Brecciated crystalline limestone	0.32	0.45	0.14	0.22	0.00	37.36
S5	Calcareous quartz schist	0.23	0.44	0.43	0.77	0.20	5.59
S6	Iron oxide cemented sandstone	0.49	0.60	0.26	0.48	0.02	11.02
S7	Carbonate cemented conglomerate	0.72	0.88	0.11	0.20	0.00	34.31
S8	Slope debris	0.88	1.45	0.04	0.08	0.00	79.07
S9	Fault breccia	0.76	1.15	0.13	0.30	0.00	18.44

Limitations: This study employed 2D plane-strain models and an analytical elastoplastic solution for probabilistic assessment; 3D effects and longitudinal variability were not explicitly modelled and should be considered in follow-up studies. Parameter distributions were defined from available data; larger sample sizes would reduce uncertainty in distribution tails.

5. CONCLUSION

This study presented a comprehensive evaluation of constitutive models and support design strategies for the Honaz Tunnel, employing a hybrid methodology that integrates field-calibrated numerical modeling with probabilistic risk assessment. Based on the comparative analysis of nine rock mass units under varying stress conditions, the following conclusions are drawn:

1. Constitutive Model Selection: The Mohr-Coulomb (MC) criterion exhibited superior performance in predicting convergences in weak, heterogeneous rock masses, achieving an exceptionally high correlation with field measurements (R^2=0.94). In contrast, Hoek-Brown-based models (HB and GHB) tended to overestimate crown convergence in weak rock mass units (e.g., slope debris), likely due to challenges in characterizing the non-linear failure envelope of extremely poor-quality rock masses under low confinement.
2. Support System Efficacy: Among the six empirical classification systems evaluated, support designs based on RMQR, Q-system, and NATM proved most effective in controlling convergence in weak ground. RSR-based designs were found to be less conservative, leading to higher predicted convergences.
3. Probabilistic Risk Insight (Novelty): The probabilistic analysis using 45,000 Monte Carlo simulations revealed critical insights that deterministic models missed. While the weakest rock mass units (S8, S9) showed low stress-induced convergence due to shallow depths, the Calcareous Quartz Schist (S5) unit emerged as the most critical section. Despite having higher mean strength than the debris units, Unit S5 presented the highest failure

probability (0.2%) and the lowest Reliability Index (β=5.59), highlighting the significant risk posed by parameter uncertainty in transition zones.

4. Design Reliability: The study demonstrates that a deterministic safety factor approach is often insufficient for tunnel design in heterogeneous geology. The integration of reliability indices (β) provided a more robust metric for assessing safety, particularly in zones where spatial variability is high.
5. Overestimated Convergences: At low GSI values (<25), the GHB criterion tends to overestimate the plastic zone around the tunnel, resulting in overestimated convergences. The MC model proved to be more suitable for this specific site, as it utilizes field-calibrated "equivalent" parameters.

In conclusion, this research suggests that for tunnels excavated in weak and variable rock masses, a "Hybrid Design Approach"—combining a simple, linear constitutive model (MC) for calibration with probabilistic frameworks for risk quantification—offers a practical and safe engineering solution. Future research should focus on extending this probabilistic workflow to 3D numerical models to capture longitudinal spatial variability more accurately.

6. REFERENCES

Aydan O, Ulusay R and Tokashiki N (2014) A New Rock Mass Quality Rating System: Rock Mass Quality Rating (RMQR) and Its Application to the Estimation of Geomechanical Characteristics of Rock Masses. Rock Mech Rock Eng 47, 1255–1276. https://doi.org/10.1007/s00603-013-0462-z

Barton N, Lien R & Lunde J (1974) Engineering classification of rock masses for the design of tunnel support. Rock Mechanics 6, 189–236. https://doi.org/10.1007/BF01239496

Barton N (2002) Some new Q-value correlations to assist in site characterization and tunnel design. Int. J. Rock Mech. Min. Sci. 39 (1), 185- 216. https://doi.org/10.1016/S1365-1609(02)00011-4.

Bienawski ZT (1989) Engineering rock mass classifications: a complete manual for engineers and geologists in mining, civil, and petroleum engineering. John Wiley & Sons. ISBN: 978-0-471-60172-2

Boukarm R, Fredj M and Saadoun A (2024) Performance Evaluation of Tunnel Support System in Jointed Rock Mass by Numerical Simulation: A Case Study. KSCE J Civ Eng 28, 1534–1545 https://doi.org/10.1007/s12205-024-0529-2

Brown ET (1970) Strength of models of rock with intermittent joints. Journal of the Soil Mechanics and Foundations Division, 96(6), 1935-1949. https://doi.org/10.1061/JSFEAQ.0001479

Carranza-Torres C & Fairhurst C (1999) The elasto-plastic response of underground excavations in rock masses that satisfy the Hoek–Brown failure criterion. International journal of rock mechanics and mining sciences, 36(6), 777-809. https://doi.org/10.1016/S0148-9062(99)00047-9

Coulomb CA (1776) “Sur une application des règles maximis et minimis a quelques problems de statique, relatives a l’architecture.” Acad Sci Paris Mem Math Phys 7:343–382.

Fama MED (1993) Numerical modeling of yield zones in weak rock. In Analysis and design methods (pp. 49-75). Pergamon. https://doi.org/10.1016/B978-0-08-040615-2.50009-5.

Hoek E, (1968) Brittle failure of rock. In Rock Mechanics in Engineering Practice. (eds K.G. Stagg and O.C. Zienkiewicz), 99-124. London: Wiley.

Hoek E and Brown ET (1980a) “Underground Excavations in Rock, London”, Instn Min. Metall.

Hoek E and Brown ET (1980b) “Empirical strength criterion for rock masses”, J. Geotech. Engng Div., ASCE 106 (GT9), 1013-1035.

Hoek E, Kaiser PK and Bawden WF (1995) Support of underground excavations in hard rock. Balkema, Rotterdam, Brookfield, p 213.

Hoek E and Marinos P (2000) Predicting tunnel squeezing problems in weak heterogeneous rock masses. Tunnels and tunnelling international, 32(11), 45-51.

Hoek E, Carranza-Torres C and Corkum B (2002) "Hoek-Brown Failure Criterion - 2002 Edition", Proceedings of the 5th North American Rock Mechanics Symposium, Toronto, Canada, Vol. 1, p. 267 -273.

Hoek E and Brown ET (2019) The Hoek–Brown failure criterion and GSI–2018 edition. Journal of Rock Mechanics and Geotechnical Engineering, 11(3), 445-463. https://doi.org/10.1016/j.jrmge.2018.08.001

Jing L (2003) "A review of techniques, advances and outstanding issues in numerical modelling for rock mechanics and rock engineering", International Journal of Rock Mechanics and Mining Sciences, Volume 40, Issue 3, Pages 283-353, ISSN 1365-1609, https://doi.org/10.1016/S1365-1609(03)00013-3.

Karakaplan E (2023) "Numerical analysis of underground engineering structures under static and dynamic conditions: The case study of Honaz Tunnel" (in Turkish), PhD Thesis, Pamukkale University, Denizli, Türkiye. https://hdl.handle.net/11499/50235

Labuz JF and Zang A (2012) ISRM Suggested method for Mohr-Coulomb failure criterion. Rock Mech Rock Eng 45:975–979. https://doi.org/10.1007/s00603-012-0281-7

Mohr O (1900) Welche Umstände bedingen die Elastizitätsgrenze und den Bruch eines Materials. Zeit Des Ver Deut Ing 44:1524–1530

Mushahary L, Deka D, Saha A, Sreedeep S (2020) Numerical Modeling of Tunnel Support Designing in Weak Rock. In: Latha Gali, M., P., R.R. (eds) Geotechnical Characterization and Modelling. Lecture Notes in Civil Engineering, vol 85. Springer, Singapore. https://doi.org/10.1007/978-981-15-6086-6_44

Palmström A (1995) RMi – a rock mass characterization system for rock engineering purposes. PhD Thesis, University of Oslo, Department of Geology, 405 p.

Rabcewicz L (1964) The New Austrian Tunneling Method. Water Power, 453-457.

Rocscience (2021) RS2 User Guide. https://www.rocscience.com/help/rs2/verification-theory, (accessed 1 March 2021).

Saeidi A, Cloutier C, Kamalibandpey A and Shahbazi A (2022) Evaluation of the Effect of Geomechanical Parameters and In Situ Stress on Tunnel Response Using Equivalent Mohr-Coulomb and Generalized Hoek-Brown Criteria. *Geosciences*, *12*(7), 262. https://doi.org/10.3390/geosciences12070262

Terron-Almenara J, Holter KG and Høien AH (2023) A Hybrid Methodology of Rock Support Design for Poor Ground Conditions in Hard Rock Tunnelling. Rock Mech Rock Eng 56, 4061–4088 https://doi.org/10.1007/s00603-023-03273-8

Terron-Almenara J, Skretting E & Holter KG (2025) Design of Rock Support in Low Overburden and Hard Rock Conditions with the use of Rock Mass Classification Systems and Numerical Analyses: a Study Based on the Construction of the Hestnes Railway Tunnel, Norway. Rock Mech Rock Eng 58, 11553–11578 https://doi.org/10.1007/s00603-024-04126-8

Wickham GE, Tiedemann HR Skinner EH (1972) Support determinations based on geologic predictions. In N Am Rapid Excav and Tunnelling Conf Proc (Vol. 1). http://dx.doi.org/10.1016/0148-9062(75)90446-5

Zhang X, Zhang D, Rong Y, Ma Y, Yao C & Sun Y (2024) Study on the stability of tunnel in weak surrounding rock considering initial support parameters and excavation method. *KSCE Journal of Civil Engineering*, *28*(6), 2427-2439. https://doi.org/10.1007/s12205-024-1520-7

Statements and Declarations

Funding: This work was supported by Pamukkale University, grant number: 2019FEBE053. **Competing Interests:** The authors declare that they have no known competing financial interests or personal relationships that could have appeared to influence the work reported in this paper. **Author Contributions:** E.K.: Conceptualization, methodology, numerical modelling, probabilistic analysis, field calibration, visualization, manuscript writing. D.A.: Supervision, project administration, funding acquisition. **Data Availability:** Data will be made available on request.